

AD-A089 701

AIR FORCE GEOPHYSICS LAB HANSCOM AFB MA

F/G 4/2,14/5

LOCAL FORECASTING THROUGH EXTRAPOLATION OF GOES IMAGERY PATTERNS.

23 SEP 80 MUENCH, STUART

UNCLASSIFIED AFGL-TR-80-0273

1-1  
1-2



END

DATE

FILED

12-81

DTIC



AD A 089701

Unclassified SECURITY CLASSIFICATION OF THIS PAGE (When Data Entered)		READ INSTRUCTIONS BEFORE COMPLETING FORM	
REPORT DOCUMENTATION PAGE			
1. REPORT NUMBER AFGL-TR-80-0273	2. GOVT ACCESSION NO. AD-A089701	3. RECIPIENT'S CATALOG NUMBER	
4. TITLE (and Subtitle) LOCAL FORECASTING THROUGH EXTRAPOLATION OF <u>GOES</u> IMAGERY PATTERNS.		5. TYPE OF REPORT & PERIOD COVERED Interim Rept.	
7. AUTHOR(s) H. Stuart Muench		8. CONTRACT OR GRANT NUMBER(s)	
9. PERFORMING ORGANIZATION NAME AND ADDRESS Air Force Geophysics Laboratory (LYU) Hanscom AFB Massachusetts 01731		10. PROGRAM ELEMENT, PROJECT, TASK AREA & WORK UNIT NUMBERS 62101F 66700804	
11. CONTROLLING OFFICE NAME AND ADDRESS Air Force Geophysics Laboratory (LYU) Hanscom AFB Massachusetts 01731		12. REPORT DATE 23 September 1980	
14. MONITORING AGENCY NAME & ADDRESS (if different from Controlling Office) 461518		13. NUMBER OF PAGES 6	
LEVEL		15. SECURITY CLASS. (of this report) Unclassified	
		15a. DECLASSIFICATION/DOWNGRADING SCHEDULE	
16. DISTRIBUTION STATEMENT (of this Report) Approved for public release; distribution unlimited.			
17. DISTRIBUTION STATEMENT (of the abstract entered in Block 20, if different from Report)			
18. SUPPLEMENTARY NOTES Presented at 8th Conference on Forecasting and Analysis, Denver, CO 10-13 June 1980, American Meteorological Society (Preprint pp 123-128)			
19. KEY WORDS (Continue on reverse side if necessary and identify by block number) Short-range forecasting Cloud motions Cloud development Satellite meteorology			
20. ABSTRACT (Continue on reverse side if necessary and identify by block number) An attractive approach to short-range forecasting is to determine cloud motion from a sequence of satellite images and extrapolate the patterns and associated weather into the future. Objective motion vector techniques are available and the forecast procedure can be accomplished by computer. This approach is being evaluated at AFGL and this report presents results of testing motion vector techniques. Tracking and covariance techniques were compared along with winds aloft and persistence (no motion) as controls. A covariance technique had top score, but only slightly better than persistence.			

DDC FILE COPY

FORM 1 JAN 73 1473

Unclassified 401578  
SECURITY CLASSIFICATION OF THIS PAGE (When Data Entered)

TR-80

Unclassified

SECURITY CLASSIFICATION OF THIS PAGE(When Data Entered)

Complicating factors and implications to forecasting are discussed.

Accession For	
NTIS GRA&I	<input checked="checked" type="checkbox"/>
DDC TAB	<input type="checkbox"/>
Unannounced	<input type="checkbox"/>
Justification	
By	
Distribution/	
Availability Codes	
Dist.	Avail and/or Special
A	23 C7

Unclassified

SECURITY CLASSIFICATION OF THIS PAGE(When Data Entered)

# 7273

## LOCAL FORECASTING THROUGH EXTRAPOLATION OF GOES IMAGERY PATTERNS

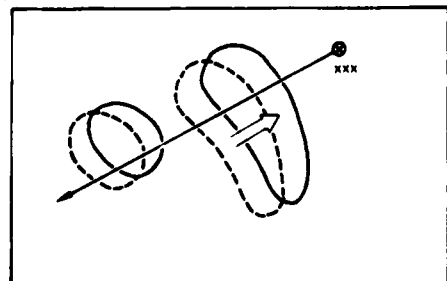
H. Stuart Muench

Air Force Geophysics Laboratory  
Bedford, Massachusetts

### 1. INTRODUCTION

The development of the geosynchronous weather satellite (GOES) has presented forecasters with the opportunity to significantly advance the art of short-range forecasting. Where the forecaster formerly had hourly surface observations from stations 100 km apart, he now can have digital satellite observations every half-hour at locations 1-km apart for video and 8-km apart for IR. In fact, the previous famine for mesoscale data has now become a feast. A single satellite transmits more numbers in a few seconds than do all the weather observers in the world in 24 hours. The problem for the forecaster is now how to digest all this information and still meet the deadlines of short-range forecasts

An attractive way to assist the forecaster is to develop an automated (or semi-automated) forecast procedure which produces guidance forecasts. An elementary procedure, based on extrapolation, is shown below in Figure 1.



TWO LATEST SATELLITE IMAGES (SUPERIMPOSED)

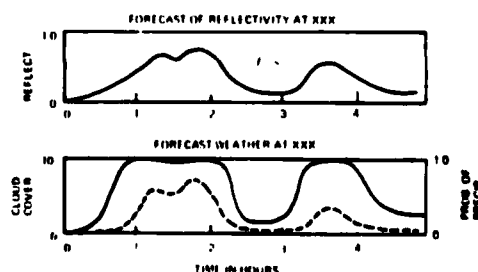


Fig. 1: Illustration of short-range forecasting, using GOES imagery data.

At the top of Figure 1 are two overlaid satellite images, the earlier image shown by dotted lines. One can use objective or subjective techniques to obtain a motion vector, as indicated by the short arrow pointing towards station XXX. To forecast for XXX, one reverses the vector and looks "upstream" increments of distance in proportion to the increments of time that are of interest. At each increment one extracts the satellite observed reflectivity from the most recent image, and the result is the forecast of reflectivity in Figure 1B. Finally one uses statistically derived algorithms to convert reflectivity to cloud cover and probability of precipitation as shown in Figure 1C.

This approach has been used with digital radar data, both by the National Weather Service and McGill University, and should be applicable to GOES imagery data. A more sophisticated version would include infrared as well as video reflectivity, and more forecast parameters. However, we should first test the concept with a simple model to determine if changes in reflectivity (hence weather) can be adequately forecast and determine where sophistication is needed to improve performance.

### 2. FIRST TEST OF MOTION VECTOR TECHNIQUES

Several objective techniques for determining motion vectors from successive satellite images have been reported in the literature. In general, these were developed to be operated interactively with a computer to measure winds aloft in regions of sparse data. However, the cloud tracking procedures of SRI (Endlich et al-1971, Wolf et al-1977) and the cross-covariance technique (Leese and Novak-1971) appear capable of operating in an automatic mode. A copy of the SRI-1977 program was obtained from the Naval Environmental Prediction Research Facility and computer programs were constructed based on journal articles for the SRI-1971 and the cross-covariance technique (using fast-Fourier-Transforms). While these programs were being prepared, a binary covariance technique was developed, which reduces the GOES image to binary values (one or zero) and computes covariance using logical arithmetic, 60 gridpoints at a time.

The following are characteristics of the four motion vector techniques (more details can be found in Muench and Hawkins, 1979):

- 1) SRI-1971  
30x30 arrays, select 100 brightest points. Identify and locate cloud centers. Match pairs, compute mean displacement.
- 2) SRI-1977  
70x70 arrays, select brightness 6 percent. Locate, identify and characterize cells. Match pairs, compute mean displacement.
- 3) fFt Cross-covariance  
32x32 arrays, convert to frequency domain. Compute covariance matrix of trial displacements. Find displacement with maximum covariance.
- 4) Binary Cross-covariance  
60x60 initial and 80x80 final arrays. Convert to binary. Sum matching 1's and 0's for trial displacements. Find displacement with maximum matches.

The first test used a 240x240 array of 2-km GOES video data as in initial array. For the final array, the initial imagery was used but artificially displaced to simulate a motion of 15 mps over  $\frac{1}{2}$  hour. Each motion vector program extracted data values so as to cover the arrays (e.g. every 7th point, every 3rd point). Six images were chosen, representing a variety of synoptic conditions, and for each image, 3 different displacements were made. In all, 18 motion vectors were computed for each technique. Some preliminary tests indicated that the SRI programs were having difficulty with fine structures, and so the 240x240 arrays were given an 8x16-point smoothing. The results of the test are shown below in Table 1.

Table 1. Test results using artificial displacements. Vector error is rms resultant error divided by artificial displacement.

	rms col. error	rms row error	Vector error
SRI-1971	$\pm 8.3$	$\pm 3.9$	$\pm 59\%$
SRI-1977	$\pm 6.0$	$\pm 3.7$	$\pm 49\%$
fFt Cross covariance	$\pm 4.9$	$\pm 3.8$	$\pm 42\%$
Binary Cross- Covariance	$\pm 0.3$	$\pm 1.5$	$\pm 10\%$

In this first test, the binary cross-covariance technique was clearly superior to the other three. An inspection of individual cases showed that all techniques worked well, vector errors 15% or less, when the brightest portion of the clouds was in the center of the array. For a variety of reasons, the first three techniques produced unreliable results when the brightest portion was on a boundary.

### 3. SECOND TEST OF MOTION VECTOR TECHNIQUES

The first test was well controlled in that the true motions were predetermined. And, the test was revealing since the boundary problems were uncovered. However, the test was not completely realistic as the consecutive images did not include the effects of cloud development and decay, as well as motion. Thus, a second test was run to check the performance of the techniques using series of consecutive half-hourly video images. The object of the test was to have each of the motion vector techniques determine motions and make forecasts of reflectivity through simple extrapolation of pattern motion. Verifications of forecasts would indicate which techniques produce the most reliable results and comparisons with a control such as persistence would indicate to what extent simple extrapolation is a useful short-range forecast procedure.

Twelve cases were selected, representing widely varying synoptic conditions, including cold fronts, warm fronts, advancing and retreating cyclonic storms. Each case consisted of six consecutive satellite video images at normally half-hourly intervals (in four cases there was a one-hour gap between two of the images). The region for which 2-km video data are archived is shown below in Figure 2.

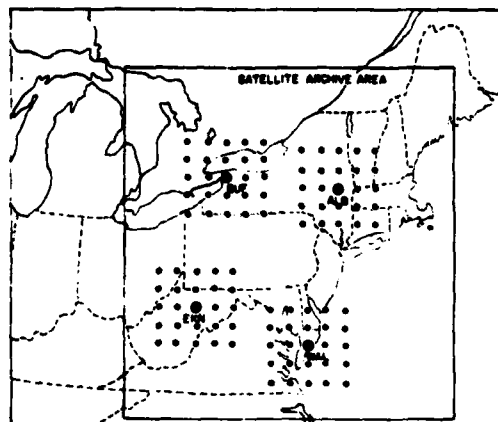


Figure 2: Satellite data archive area, locations of motion vector points, and grid of points used for forecast and verification.

Four techniques were added to those used in the first test. A variation was made on the fFt cross-covariance to have a larger 48x48 initial array in hopes of alleviating the boundary problem, through risking aliasing problems. For controls, two radiosonde winds aloft were included, the 1200 UT 700mb level wind and  $\frac{1}{2}$  the 500mb level wind. These winds are sometimes used to "steer" radar patterns and developing storms. The last control added was "persistence" or no local change with time, a control that is often difficult to beat in short range forecasts.

The five motion vector programs using satellite data computed motion vectors at each of the four locations shown in Figure 2, for each consecutive pair of images in each of the 12 cases. A 25-pt array, with 64-km spacing, was set up over each location to serve as the forecast and verification points.

In order to assure correct positioning of the satellite data, a two stage "navigation" procedure was used. The basic satellite attitude and orbital parameters are refined daily, using NESS bulletins and minimizing differences between predicted and observed locations of prominent geographic features (usually in Mexico, Venezuela or Bolivia). This navigation procedure is carried out on the AFGL McIDAS system (computer interactive graphics), and overall gives positioning accuracy of about  $\pm 20$  km in the NE United States. A "fine tuning" of each archived image is performed using identifiable landmarks, within the region shown in Figure 2, which reduces the positioning error to about  $\pm 5$  km.

Varying sun angle causes problems when one uses satellite video data quantitatively, and measures were taken to correct for sun angle. Within a case, each image was normalized to noon (EST) of that a day, through use of a factor determined by comparing the histograms of reflectivity. Four reflectivity thresholds were selected to verify forecasts, 0.30, 0.55, 0.75, and 0.90, normalized to overhead sun. For each case, the thresholds were adjusted to the noontime sun, using an anisotropic scattering routine described in Muench and Keegan (1979).

The forecasts and verification were made by reversing the specified motion vector and computing the "upstream" locations at intervals equivalent to half-hour linear motion, out to 2½ hours. The forecast reflectivity consisted of an average of the four nearest 2-km resolution satellite values (normalized to local noon). With respect to each of the thresholds, forecast and verification reflectivity were either below or else equal to or above the threshold. Scores were kept of the numbers of times both forecast and verification were in the same category and numbers of times they were not. The scores were summed over all cases and final results presented in terms of percent correct. In addition, skill score relative to persistence,  $SS_p$ , was computed by:

$$SS_p = (F - P) / (1 - P)$$

where  $F$  is percent correct for the motion vector technique and  $P$  is the percent correct for persistence. Results summed over all forecast time intervals and all thresholds are shown below in Table 2 (More completed results can be found in Muench-1979).

Table 2. Percent Correct and Skill Scores of Forecasts from Motion Vector Techniques. Twelve cases, all time intervals and all thresholds combined.

Technique	Percent Correct	Skill Scores
Satellite-based motion vectors		
SRI-1971(AFGL)	0.880	-0.16
SRI-1977	0.892	-0.05
fFt(1) Covariance	0.897	0.00
fFt(2) Covariance	0.900	0.03
Binary Covariance	0.903	0.06
Controls		
700-mb	0.900	0.03
½ 500 mb wind	0.898	0.01
Persistence	0.897	0.000

Among the satellite-based techniques, the relative standings are exactly as they were in the first test, with the best score for the binary covariance, followed by the fFt-covariance techniques, then the SRI-1977 and finally the SRI-1971. In Figures 3 and 4 (following page) the relative positions are essentially the same for all time intervals and all thresholds, so even though the differences are small, the results appear stable. In the lower part of Table 2, one notes that the two upper-wind controls scored nearly as well as the covariance techniques, raising the question whether the effort of computing covariance motion vectors can be justified in regions where radio-sonde data are plentiful.

The most important point in Table 2 and Figures 3 and 4 is that none of the techniques is much better than simple persistence. This becomes readily apparent by examining the skill scores in Table 2, which indicate some are actually negative. While the percent correct for persistence is quite high, leaving little room for improvement, never-the-less, the best of the motion vector techniques correctly forecasted less than one of every sixteen threshold crossings that occurred.

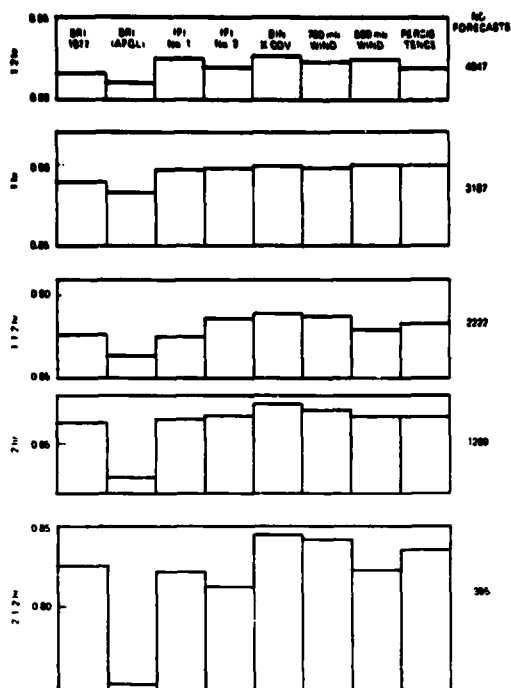


Figure 3. Percent correct for forecasts by time intervals (4 thresholds combined).

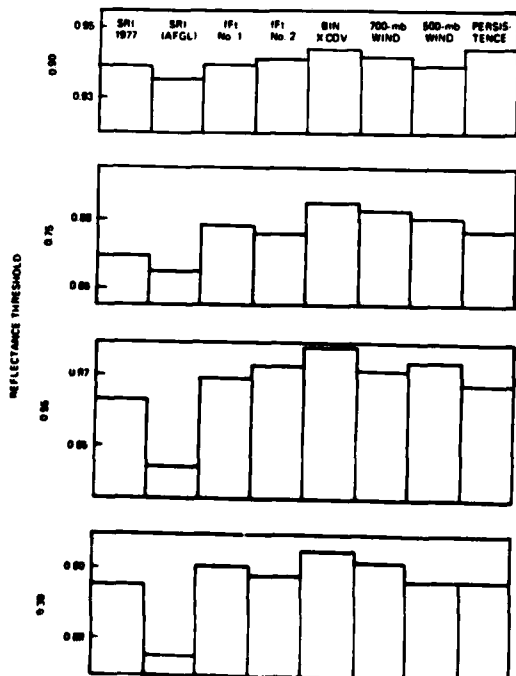


Figure 4. Percent correct for forecasts, by threshold (5 time intervals combined).

The first thought upon seeing the small skill scores was that there were programming or navigation errors. However, a thorough check showed that this was not the case.

Next, there was concern over the use of 4x4km (2x2 mile) average reflectivity in the forecasts and verification. Most cloud cells as small as 4km could not be expected to have a life-span more than  $\frac{1}{2}$  hour, and those that did would require very precise determination of motion to be correctly forecast, particularly when speeds were greater than 10mps. So, the forecast-verification program was re-run, only a 23x23km (13x13 mile) smoothing was applied to the reflectivity data. However, the resulting scores were again nearly the same as persistence. Figure 5 shows the variation of percent correct with time for both persistence and the binary cross-covariance technique, with the lower curves for 4x4km run and the upper curves for the 23x23km run. The principal effect of the smoothing was to increase the percent correct for persistence at all time intervals, with a nearly identical increase for the covariance technique. Apparently, the larger disturbances remaining after the 23km smoothing were just as difficult to forecast as the smaller ones filtered out.

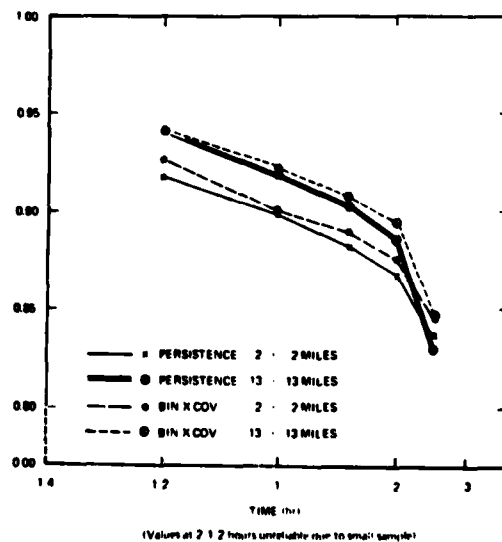


Figure 5. Percent correct versus time, for binary cross-covariance and persistence, for 4x4km average data and 23x23km average data.



4.

#### DIAGNOSIS OF PROBLEMS

An obvious conclusion from the second test is that the simple extrapolation forecast scheme illustrated in Figure 1 will not produce forecasts substantially better than persistence. While we might consider trying to improve the motion vector techniques, at this point it would be prudent to perform a more complete diagnosis to see if perhaps the scheme is too simple and that more sophistication is required.

An examination was made of a case on 15 Nov. 1977. A weak cold front had passed through the northeast the previous day, leaving an eastwest quasi-stationary front across the Virginias. While there was still cold air advection in the lower levels over New England, a weak upper level trough was moving rapidly eastward from the Mississippi Valley, along with a slowly developing wave on the front.

Normalized reflectivity values were extracted for 31x41 arrays of 10km average data over each of the stations shown in Figure 2. Similar arrays were also obtained for infrared "temperature" and reflectivity standard deviation. Surface observations and radiosonde ascents were analyzed to determine the three-dimensional cloud structure and its variations with time.

An example of an analysis of the reflectivity field around station ALB is shown below in Figure 6. In the lower right, the skies were essentially clear, while to the northwest clouds prevailed. Over the hills of Vermont and New Hampshire were heavy stratocumuli that were stationary, such as the stippled areas marked "A". However, a clear area in northeast New York state, marked "B" was spreading steadily south and east during the day and eventually the clouds over the mountains disappeared. Obviously, no single motion vector could correctly forecast the features A and B.

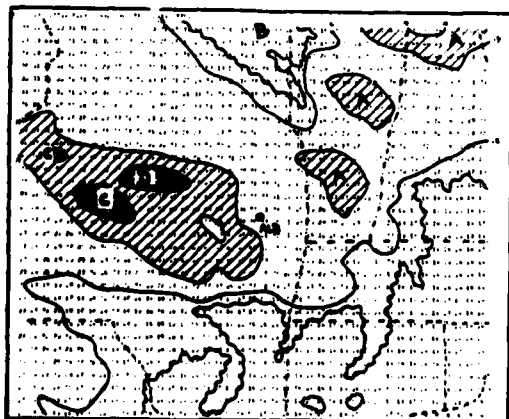


Figure 6: Analysis of reflectivity in vicinity of station ALB, at 1700 UT, 15 Nov 1978.

To the west of station ALB, another complication was found. The heavy stippled areas marked "C" were the most intense portion of a stationary pattern that extended southeast from Lake Ontario. These were basically low clouds with considerable vertical development, including rain showers. Above, there was a layer of cirrus that had spread eastward to near ALB, and imbedded in the cirrus was a dense area marked "D" that was moving east at 30 to 35 mps. Again, no single motion vector could forecast these independent motions.

Figure 7, below, shows another analysis of the reflectivity, near station WAL in the Del-Mar-Va peninsula. In this region there was an extensive area of middle and high clouds that was spreading eastward, and rain was associated with the stippled area clouds. A few holes in the clouds were present in the upper right (northeast) portion. The reflectivity pattern was quite complex in form, and as might be expected, the forms changes from image to image. Part of the change was due to a systematic weakening of the most intense areas as they moved east-northeastward. Other changes have not yet been diagnosed. Such changes would lower the scores of extrapolation based forecast techniques. Also, within this area, the patterns in the upper left were moving noticeably faster than those in the lower right, and a single motion vector was not adequate.



Figure 7: Analysis of reflectivity in vicinity of station WAL, at 1700 UT, 15 Nov 1978.

As more cases are analysed, undoubtedly other complicating factors will be found. However, at this point it is clear that a successful forecast technique will have to include a means to cope with patterns with different motion, close to each other or even superimposed. A partial solution is to perform a vertical separation of the cloud layers, using all available data, and forecast each layer separately.

We should keep in mind that the satellite imagery from clouds is merely a manifestation of vertical air motion in a moist environment. The cloud particles grow and fall sufficiently fast that images an hour or more apart are not viewing the same particles. In essence, when we forecast the future cloud patterns, we are forecasting the vertical motions. So, one would do well to keep the dynamics and physics in mind when developing satellite-based forecast techniques.

### 5. SUMMARY AND CONCLUSIONS

To utilize geosynchronous satellite information in short-range forecasting, a simple extrapolation procedure was proposed. Successive imagery data would be used to compute a motion vector. Next, the motion vector would be used to predict the time history of reflectivity at a point. Finally, algorithms would translate the reflectivity forecast to common weather parameters.

Test were run to find the most suitable means to compute motion vectors. In the first test, using specified motions, the techniques described in the literature worked well only when the brightest portion of the pattern was in the center of the working array. A binary-cross-covariance technique worked well for all conditions. In a second test, making reflectivity forecasts, again the binary cross-covariance scored best, but the differences were small. The scores of the upper-level winds were very nearly as high as the covariance scores. None of the techniques improved substantially upon the scores of persistence.

The failure to improve over persistence casts doubts upon the suitability of simple extrapolation as a short-range forecast technique. An analysis was made of cloud structure and evolution at several locations. Several complicating factors were found, including moving and stationary patterns in close proximity, sometimes at the same level in the vertical, and sometimes at different levels.

While it was disheartening to see that simple extrapolation was scarcely better than persistence, the problems can be diagnosed with the aid of the geosynchronous satellite data. Since the problems can be diagnosed, the construction of a successful short-range forecast procedure should be possible.

### REFERENCES

1. Endlich, R.M., D.G., Wolfe, D.J. Hall, and A.G. Brain, 1971: The Use of Pattern Recognition Techniques for Determining Cloud Motions from Sequences of Satellite Photographs, J. Appl. Meteor., 10, 105-117.
2. Leese, J.A. and C.S. Novak, 1971: An Automated Technique for Obtaining

Cloud Motion from Geosynchronous Satellite Satellite Data Using Cross-correlation, J. Appl. Meteor., 10: 118-132.

3. Muench, H.A. and R.S. Hawkins, 1979: Short-Range Forecasting through extrapolation of satellite imagery patterns, Part I: Motion vector techniques, Air Force Geophysics Laboratory, AFGL-TR-79-0096(NTIS AD/A073081).
4. Muench, H.S. and T.J. Keegan, 1979: Development of techniques to specify cloudiness and rainfall rate using GOES imagery data. Air Force Geophysics Laboratory, AFGL-TR-79-0255, (copies available from authors, AFGL/LYU, Hanscom AFB, Bedford, MA 01731).
5. Muench, H.S., 1979: Short-range forecasting through extrapolation of satellite imagery patterns, Part II: Testing motion vector techniques, Air Force Geophysics Laboratory, AFGL-TR-79-0294(copies available from author, AFGL/LYU, Hanscom AFB, Bedford, MA 01731).
6. Wolf, D.E., D.J., Hall, and R.M. Endlich, 1977: Experiments in automatic cloud tracking using SMS-GOES data. J. Appl. Meteor., 16: 1219-1230.